JOURNAL OF APPLIED ELECTROCHEMISTRY 22 (1992) 1031–1038

Raney nickel activated H_2-cathodes Part II: Correlation of morphology and effective catalytic activity of Raney-nickel coated cathodes

Th. BORUCIŃSKI, S. RAUSCH, H. WENDT

Institut für Chemische Technologie, TH Darmstadt, Petersenstrasse, 20, D-6100 Darmstadt, Germany

Received 2 December 1991; revised 2 April 1992

Raney nickel activated hydrogen-cathodes obtained by caustic leaching of cathodically deposited Ni/Zn precursor alloy coatings on nickel substrates were investigated with respect to their effective catalytic activity. Important factors influencing this activity are the surface specific amount of the inner surface of the Raney nickel coatings and, in particular, the tertiary structure of the catalyst coating. Coarse pores and cracks are developed during leaching of the Ni/Zn precursor which, due to unsteady deposition conditions, show a layered structure. These cracks are essential for a high catalytic activity, since micropores of Raney nickel coatings are utilized to pore depths of no more than 10 μm. The generation of layered structures of the coatings with changing zinc content, which is experienced by Ni/Zn codeposition from acidic solutions, is influenced by a number of process parameters. The most important parameter is the cathode potential which may fluctuate strongly during cathodic deposition of the Ni/Zn precursor coatings due to minute temperature and/or pH changes.

1. Introduction

1.1. *Raney-nickel coatings*

The catalytic activation of hydrogen evolving cathodes by Raney-nickel coatings used for catalyzing cathodic hydrogen gas evolution in caustic electrolytes (for example in chloralkali electrolysis and for alkaline water electrolysis) has a long tradition. The principle of this electrocatalyst is its high internal surface, amounting to approximately 100 $m^2 g^{-1}$ [1]. Figure 1 illustrates several procedures for applying leachable Raney-nickel precursor alloys ($NiAl_3/Ni_2Al_3$ or Ni/Zn alloys) to the surface of supporting nickel or stainless steel cathodes. For very active Raney-nickel coatings, at which cathodic overpotentials of no more than 100 mV at current densities of 1000 mA cm^{-2} and temperature of 100 °C in 40 wt % KOH prevail, only nickel supports can be used since neither mild steel nor stainless steels are reliably passivated at such low cathodic potentials at which iron is no longer immune [2].

Cold rolling and plasma spraying of Raney-nickel precursor alloys on to the nickel support has been proposed, as well as the formation of the prealloys by annealing aluminium or zinc-coated electrodes, which leads to the formation of layers of Ni/Al or Ni/Zn alloys of variable composition by interdiffusion of Ni and Al or Ni and Zn, respectively. Cathodic deposition of Ni/Zn precursor alloys is unique as codeposition of the constituents and precursor alloy formation is performed in one single step, according to a specific codeposition mechanism. Only cold rolling of a mixture of Mond nickel and Raney-nickel [3] and the cathodic deposition of nickel–zinc alloys [4–6] are currently used commercially.

This paper deals with an investigation of the effective catalytic activity of Raney-nickel catalysts obtained by caustic leaching of galvanically codeposited Ni/Zn coatings from acidic solutions on supporting perforated nickel cathodes. Such catalytically activated cathodes are usually used in zero gap cells of advanced alkaline water electrolyzers [7–9].

Application of Raney-nickel coated electrodes means making use of the inner surface of these highly porous materials, thus drastically lowering the true current density at the inner surface of the coating, with correspondingly reduced overpotential. By using Raney-nickel coated cathodes with surface specific inner surfaces of the order of $a^* = 10^4 cm^2 cm^{-2}$ the true current density in the pores may be decreased ten thousand fold. That is,

$$i_{pore} = i_{effective}(a^*)^{-1} = 10^{-4} i_{effective} \quad (1)$$

provided the inner surface is fully used. In a previous theoretical study [10] it was shown that the latter is usually not the case for Raney-nickel coatings of 50–100 μm thickness. Recently Divisek and coworkers [11] reported on the production of Raney-nickel coated cathodes by cathodic deposition of nickel/zinc precursor alloys from chloride electrolytes. The authors did not report on layered deposition of different Ni/Zn-phases which is typical for this type of coatings. This paper reinvestigates this procedure and stresses the occurrence of layered Ni/Zn-coatings, which, by their very nature, representing layers containing either less

0021-891X © 1992 Chapman & Hall

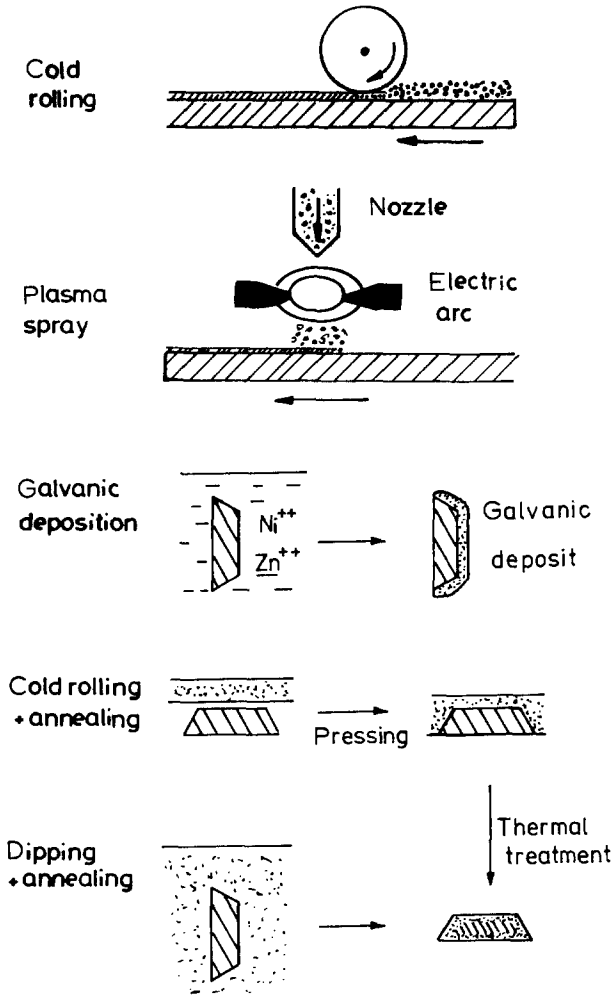

Fig. 1. Schematic presentation of several procedures for applying leachable Raney-nickel precursor alloys to the surface of supporting nickel or stainless steel cathodes.

than 30 wt % or more than 70 wt % zinc, influence the effective catalytic activity of the coating very strongly.

2. Experimental details

2.1. *Preparation of Ni/Zn precursor coatings*

As supports for the cathodic deposition of Ni/Zn precursor alloys perforated nickel sheets (VECO, sheet Type 12½ H) with a hole surface fraction of 41%, a hole diameter of 1.35 mm and a thickness of 0.24 mm were used. From these sheets pieces of 6.6 cm^2 were cut and, to their flat reverse side (the holes on the front side are tapered), two nickel wires (2 mm diam.) were point soldered; these served simultaneously as electrode holder and current lead. The perforated plate and a nickel plate of the same size serving as soluble anode were aligned parallel to each other and kept at a distance of 5 cm by polyethylene studs. Both electrodes were inserted vertically in a well stirred beaker which contained the plating bath. During the galvanic deposition of nickel zinc coatings the cathode potential, the temperature and the pH of the solution were monitored. As a reference a saturated Ag/AgCl-electrode was used. The volume of the plating bath amounted to 2000 cm^3.

For the plating solution, a chloride bath containing 1.1 M $NiCl_2$, 1.1 M $ZnCl_2$ and 0.5 M H_3BO_3 was used; in some cases various additives were added.

Since the maximum amount of zinc which was deposited did not exceed 6.5 g, the zinc content of the bath was never depleted by more than 9%, whereas the nickel concentration remained virtually unchanged due to anodic dissolution of the nickel anode which proceeded with current efficiencies between 95 and 103%, determined by weight loss of the anode.

Prior to deposition of the Ni/Zn precursor alloy the nickel supports were etched for 10 min in 5 M HCl containing 0.3 M H_2O_2. These electrodes were then rinsed, dried and weighed. Immediately before inserting them into the preplating bath they were immersed, together with the anode, in 0.1 M HCl solution where, for 10 min, hydrogen was evolved. After rinsing, a nickel layer of approximately 15 mg cm^{-2} was applied by depositing nickel with a current density of 33 mA cm^{-2} for 30 min from an acidic plating bath containing 240 g dm^{-3} $NiSO_4 \cdot 6H_2O$, 40 g dm^{-3} $NiCl_2 \cdot 6H_2O$ and 30 g dm^{-3} H_3BO_3 [12]. The anode and cathode were then immediately immersed into the Ni/Zn plating bath.

Predepositing nickel served the purpose of preparing a fresh, non-oxidized nickel surface on which the Ni/Zn alloy could be deposited in order to ensure a good adherance of the coatings to the substrate. The electrodes were weighed after deposition in order to determine current efficiencies of cathodic deposition and anodic dissolution, respectively.

2.2. *Characterization of cathodically deposited Ni/Zn precursor alloys and leached Raney-nickel coatings*

The thickness of the precursor coatings, and the thickness of the leached coatings were determined by gravimetry and microscopic investigation of etched and polished cuts. The chemical composition of the coatings was determined by complete dissolution of substrate and coating with subsequent analysis of zinc (atom absorption spectroscopy, AAS). Since the zinc of the α-phase cannot be leached by caustic potash 'leachable' zinc is distinguished from total deposited zinc content of the deposit by analytic and gravimetric determination of the amount of zinc which is leached out by 40 wt % KOH with a final leaching temperature of 90 °C, sustained for 5 h. In order to determine the effective catalytic activity of the coatings, current voltage curves of cathodic hydrogen gas-evolution were measured in 40 wt % KOH and at different temperatures, preferentially at 100 °C. An additional characterization of the morphology and coarse structure of the leached electrodes was performed by scanning electron microscopy.

2.3. *Determination of the electrochemically active inner surface of Raney-nickel coatings*

The internal surface of the Raney-nickel coating, defined by the oxidizable amount of nickel per cm^2 of electrode, was determined by coulometric oxidation

achieved by galvanostatic ($7\,mA\,cm^{-2}$) potential-monitored oxidation of the inner surface of the Raney-nickel up to a potential of $-400\,mV$ against Hg/HgO (30 wt % KOH) was reached. During this procedure all hydrogen adsorbed on the inner surface of the Raney-nickel coating and the nickel surface is oxidized. Assuming a stoichiometry of Ni/H = 1 for adsorbed hydrogen and the consumption of three electrons per Ni–H surface group, then

$$Ni\text{–}H + 3OH^- \longrightarrow Ni(OH)_2 + H_2O + 3e^- \quad (2)$$

The internal surface of the coatings can be estimated from the anodic charge, Q, of the oxidation. A reasonable estimate of the spatial demand of Ni–H groups can be obtained from the molar volume of bulk nickel, approximately $5.5 \times 10^{-16}\,cm^2$, so that a charge of $Q = 1\,Cb$ would correspond to $(1 \pm 0.1) \times 10^3\,cm^2$ total pore surface [13].

2.4. *Current voltage curves and long term performance tests of Raney-nickel activated cathodes*

All electrochemical investigations were performed in 40 wt % KOH at a temperature of 100 °C. Long term performance tests and measurements of current voltage curves of hydrogen cathodes were performed in an all PTFE-beaker, with a volume of 1 dm^3, equipped with a PTFE-reflux condenser. As a reference, a reversible hydrogen electrode (RHE) was used. The tip of the PTFE Luggin capillary of the reference electrode was arranged at the reverse side of the working electrode with a distance of less than 1 mm. Checking the measured electrode potential by the current interruption technique showed that up to current densities of $700\,mA\,cm^{-2}$ error due to the *IR*-drop did not exceed 5 mV; at $1000\,mA\,cm^{-2}$ the systematic error of measurements, without *IR*-correction, by current interruption amounted to $(25 \pm 2)\,mV$.

The long term performance tests were executed at a current density of $250\,mA\,cm^{-2}$; these tests were interrupted at regular intervals only for the current–voltage curve measurements.

3. Kinetic and thermodynamic conditions for the formation of Ni/Zn coatings with high zinc content

3.1. *Cathodic deposition of nickel zinc alloys on nickel substrate by anomalous codeposition*

The electrodeposition of Ni/Zn alloys is of the anomalous codeposition type [14, 15]. In anomalous codeposition an electrochemically less noble metal is codeposited with a nobler one at variance to thermodynamic expectation. A generalized plot of the electrodeposited alloy composition against current density which is typical for a normal codeposition is shown in Fig. 2. At low current densities (region I) the ratio of the concentration of the less noble to the more noble metal in the deposit is, as expected, smaller than in the electrolyte. The current efficiency in region I is low provided the more noble metal, in the present case

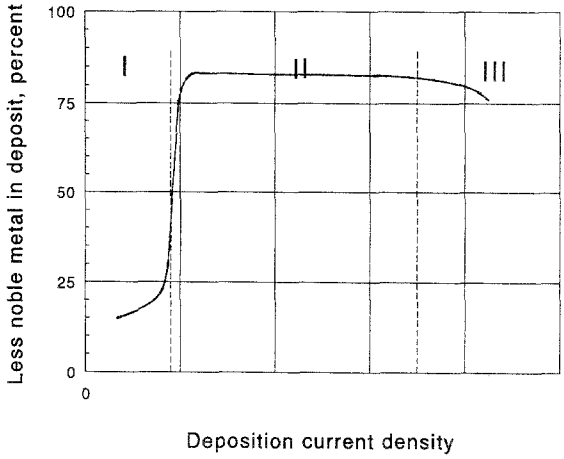

Fig. 2. Typical correlation of deposit composition and current density in anomalous codeposition.

nickel, exhibits a particularly low hydrogen overpotential and much hydrogen is evolved during metal deposition. Between regions I and II there is an abrupt transition in deposit composition and in region II the concentration of the less noble metal is higher in the electrodeposited alloy than in the bath. This phenomenon is termed anomalous codeposition. There is little change in deposit composition across region II over a broad current density range.

At still higher current densities, in region III, the content of the less noble metal decreases gradually because of increasing mass transfer limitations for the less noble metal. The current efficiency in regions II and III is high because the less noble metal, for instance zinc, exhibits a sufficiently high hydrogen overpotential; thus almost no hydrogen is evolved.

Anomalous codeposition of nickel and zinc had been explained by the so-called hydroxide suppression mechanism [14]. In region I the most noble components, hydrogen and nickel are deposited preferentially with a low current efficiency for the metal. At the transition current density, due to strong hydrogen-evolution, the pH at the cathode surface is believed to rise sufficiently to form hydroxide ions of significant concentration at the cathode. As a consequence zinc hydroxide is formed and adsorbed on the cathode and inhibits nickel deposition and simultaneously hydrogen evolution. In region II zinc deposition by cathodic reduction of adsorbed zinc hydroxide is believed to occur. In region III diffusion no longer supplies the cathode with sufficient zinc to maintain the deposit composition of region II. Therefore, in region III, increasing the deposition current density leads to a gradual drop in the fraction of the concentration of zinc metal in the deposit.

Since the deposition of nickel is believed to be retarded by zinc hydroxide formed on the cathode due to the pH increase in the cathode layer, any change in plating conditions which influences the pH in the vicinity of the cathode (convection, temperature or buffer capacity) affects the transition current density at which deposition switches from normal to anomalous.

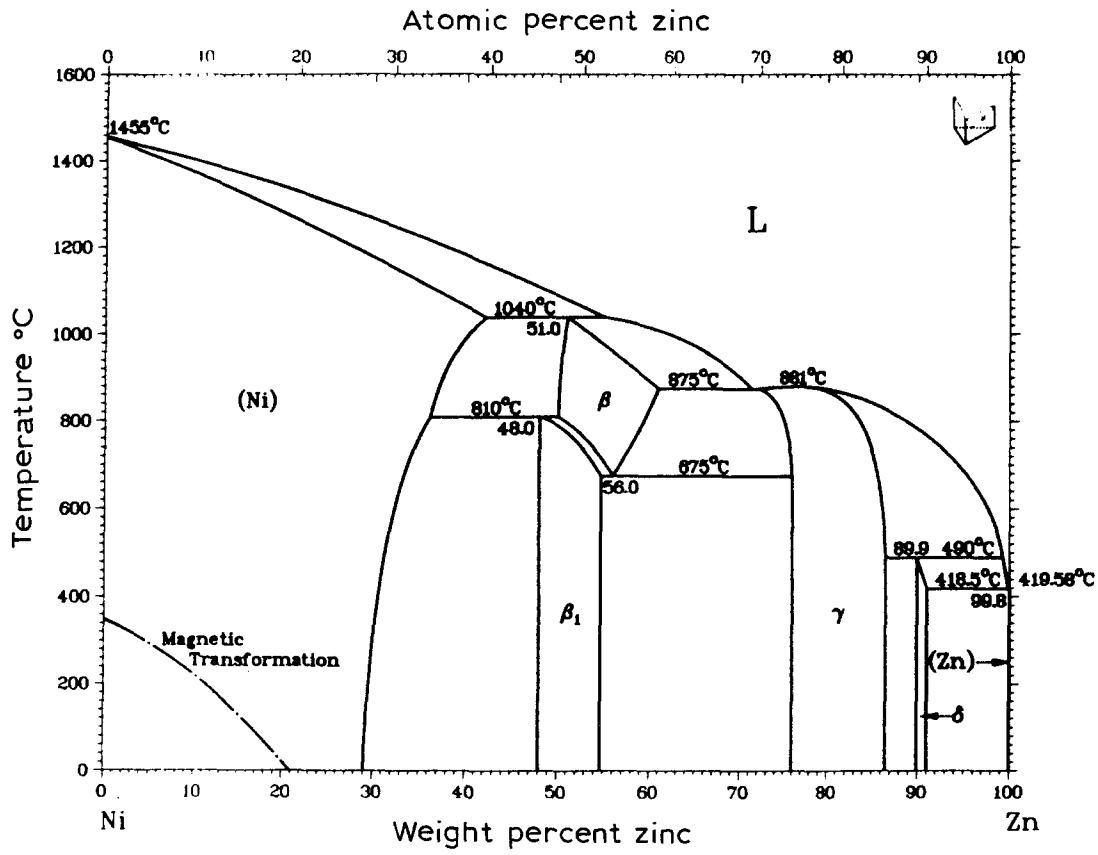

Fig. 3. The phase diagram of the binary nickel/zinc system.

3.2. *Phase diagram Ni/Zn and leaching behaviour of different Ni/Zn phases*

Figure 3 represents the phase diagram of the binary Zn–Ni system [16]. At room temperature the α-phase may contain from 0 to 27 mol % Zn. Between 45 to 52 mol % of Zn the β_1-phase is formed, from 74 to 85% Zn the γ-phase and from 89 to 90% the δ-phase exists.

In the literature only the cathodic deposition of α-phase in region I and of γ-phase and δ-phase in region II are reported. The cathodic deposition of the β_1-phase was never obtained [14, 15]. Only from the γ and the δ-phase, with more than 74 mol % zinc, can zinc be removed by caustic leaching. Leaching of the α or β_1-phase is not possible even with anodic potentials [17].

A general feature of comparable binary alloys of a non noble and a more noble metal, like Ni/Al or Ni/Si, is that the latter can only be leached by selective corrosion if the less noble metal has a volume fraction of more than 50%.

4. Results

4.1. *Performance of Ni/Zn alloy deposition from acidic Ni/Zn baths*

Some initial experiments showed that only nickel zinc coatings with a mean zinc content of the Ni/Zn prealloys of 50% or less are mechanically stable after leaching. Therefore it is important to deposit a mixture of α and γ or δ-phase with an averaged zinc content of 50%. In the first experiments the α-phase was deposited in region I (low current density and more anodic potential) and a mixture of the γ and δ-phase in region II (enhanced current density and more cathodic potential). Any minor change in plating conditions which influences the pH near the cathode surface only slightly had a drastic effect on the cathode potential and, therefore, on the deposit composition. Cathode potentials of more than −900 mV correspond to anomalous deposition with formation of γ and/or δ-phase, whereas potentials of less than −700 mV correspond to normal deposition and formation of the α-phase.

As shown in Fig. 4 for a galvanostatic experiment with a constant current density of 50 mA cm^{-2} the cathode potential is very sensitive to small changes in

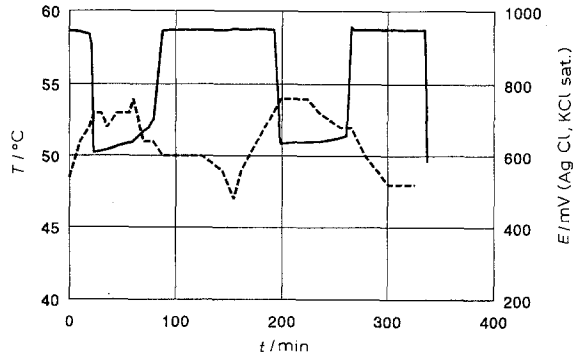

Fig. 4. Potential changes during cathodic deposition of Ni/Zn coating (electrode 6; see Table 1) in a galvanostastatic experiment (c.d.: 50 mA cm^{-2}). Changes of temperature and cathode potential are correlated. (——) E/mV and (– – –) T/°C.

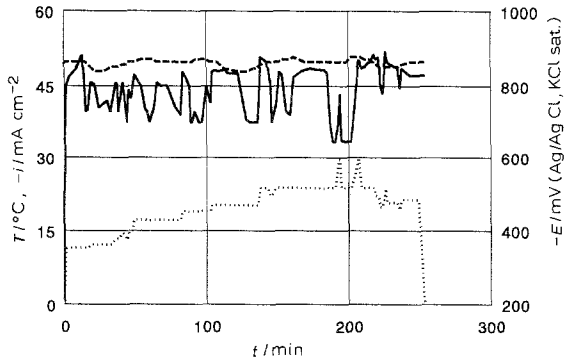

Fig. 5. Preparation of electrode 7 by an experiment with discontinuously increasing current density. The bath pH was kept constant (pH 2) by adding small amounts of acid. These additions of small amounts of acid repeatedly cause a temporary drop of cathode potential from −900 to −650 mV. (——) $-E$/mV, (– – –) T/°C and (· · ·) $-i$/mA cm^{-2}.

bath temperature. In the bath temperature range of 47 °C to 53 °C the cathode potential jumps back from −950 mV (Ag/AgCl) to approximately −600 mV; that means from anomalous to normal codeposition, with corresponding increase of the nickel content of the alloy if the temperature decreases below 52 °C. This, in turn, gives rise to reduced current efficiencies. Figure 5 shows for a deposition under discontinuously increasing current density, that the cathode potential is not simply determined by the applied current density. In this case the pH of the bath was kept constant at a value of 2 ± 0.1 by repeated addition of small quantities of acid. These small amounts of added acid obviously cause a temporary decrease in pH in the cathode layer with subsequent α-phase deposition at cathode potential of −650 mV. From this situation the cathode recovers after some minutes, returning to a potential of −900 mV with subsequent deposition of γ and/or δ-phase which possesses high hydrogen overvoltage. Fluctuations in mass transfer rates induced by changing the stirring rate generate sudden changes in the cathode potential between the two limiting potential niveaus of −600 mV to −650 mV (normal codeposition, region I) and −850 mV to −950 mV (anomalous codeposition, region II) and corresponding composition and phase changes of the deposit.

Table 1. Electrolyte composition, mass of the deposited precursor alloy, leachable zinc content of the precursor alloy and cathodic current efficiency for acidic solution

Electrode No.	*Electrolyte No.**	*Precursor-alloy* /mg cm^{-2}	*Leachable Zn content* /%	*Cathodic current efficiency* /%
1	1	53	58	60
2	1	58	62	55
3	2	54	57	62
4	1	58	2	62
5	1	63	2	65
6	1	262	45	78
7	1	44	27	45
8	1	43	28	77
9	1	43	25	76
10	3	27	45	53
11	1	28	23	52
12	1	57	11	78
13	1	57	12	79
14	1	40	30	60
15	1	41	30	63
16	1	64	15	74
17	1	64	14	74
18	1	137	13	95
19	1	139	10	93
20	1	94	35	86
21	1	4	34	86
22	4	19	28	53

* *Electrolyte 1*: 1.1 M $NiCl_2$, 1.1 M $ZnCl_2$, 0.5 M H_3BO_3; *Electrolyte 2*: 0.2 M $NiCl_2$, 0.9 M $NiSO_4$, 1.1 M $ZnCl_2$, 0.5 M H_3BO_3; *Electrolyte 3*: 1.1 M $NiCl_2$, 1.1 M $ZnCl_2$, 0.5 M H_3BO_3, gelatine; *Electrolyte 4*: 1.1 M $NiCl_2$, 0.15 M $ZnCl_2$, 0.5 M H_3BO_3.

Table 2. Comparison of the mean overpotentials of all 22 Raney nickel activated electrodes (Table 1) and the overpotential of a non activated nickel cathode, measured at 100 °C in 40 wt % KOH at current densities of 0.1, 0.25, 0.5 and 1.0 A cm^{-2}

Current density /A cm^{-2}	*Average overpotential* /V	*Overpotential of smooth nickel cathode* /V
0.1	0.08	0.21
0.25	0.15	0.27
0.5	0.20	0.31
1.0	0.28	0.37

In order to obtain an empirical basis, 22 codeposition experiments were performed with four different plating baths.

Table 1 shows electrolyte composition together with mass of the deposited precursor alloy, the leachable zinc content and the current efficiency of the deposition of the Ni/Zn layers from acidic Ni/Zn baths. All coatings can be leached and yield tough, well adhering and catalytically active Raney-nickel layers.

4.2. *Characterization of the catalytic activity of leached Ni/Zn-coatings by measurements of current–voltage curves for cathodic hydrogen evolution*

All 22 coatings exhibit increased catalytic activity after leaching compared to smooth nickel cathodes. The effective catalytic activity, the composition of the nickel zinc coating and the coating morphology varied broadly.

Table 2 shows the arithmetic mean of the overpotentials for the 22 electrodes and the overpotentials of a smooth nickel electrode at 0.1, 0.25, 0.5 and 1.0 A cm^{-2}, measured at 100 °C in 40 wt % KOH, in order to show that the mean value of the overpotential

Table 3. Difference between total and leachable zinc content for three electrodes

Electrode No.	*Leachable Zn content (AAS)* /%	*Total Zn content (AAS)* /%
19	10	23
21	34	53
22	28	44

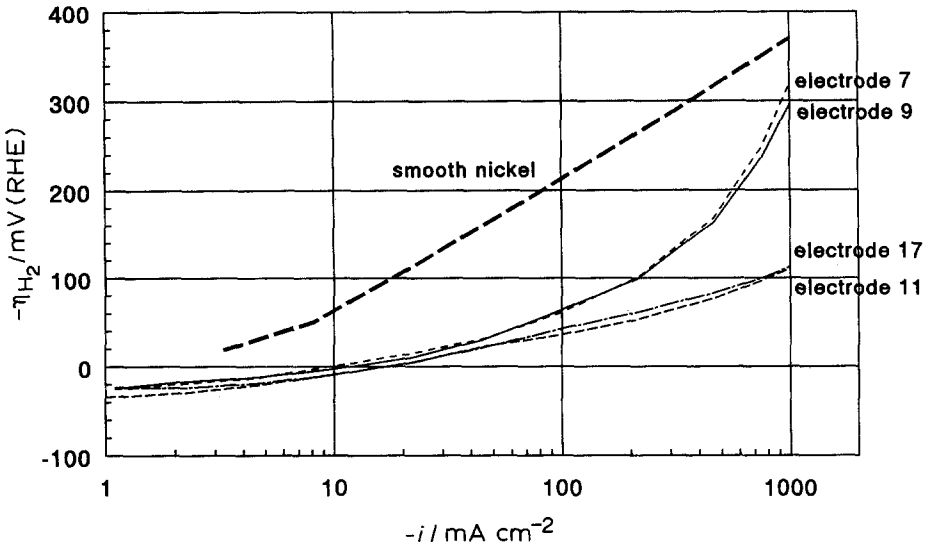

Fig. 6. Current–voltage curves of four activated hydrogen evolving cathodes (No.'s 7, 9, 11, 17) measured in 40 wt % KOH at 100 °C. As reference the i–V curve of a smooth hydrogen evolving nickel cathode is also depicted.

of these electrodes is much lower for coated than for non-coated electrodes. At high current density the average electrode, however, is not much better than non-activated electrodes. It is obvious that this failure of the effective catalytic activity at high current density is due to inappropriate morphology of the coatings rendering the inner surface of the porous catalyst inaccessible due to concentration polarisation and current blocking due to bubble formation.

Table 3 compares, for three different electrodes, obtained from acidic solutions, the difference between leachable and total zinc content. Cathode No. 19 is typical, for a coating obtained from acidic solutions, in so far as the lower the zinc content of the deposit,

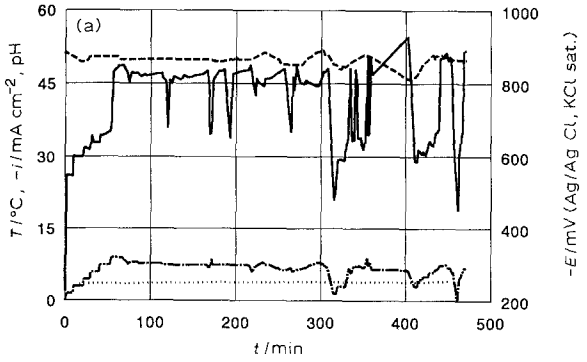

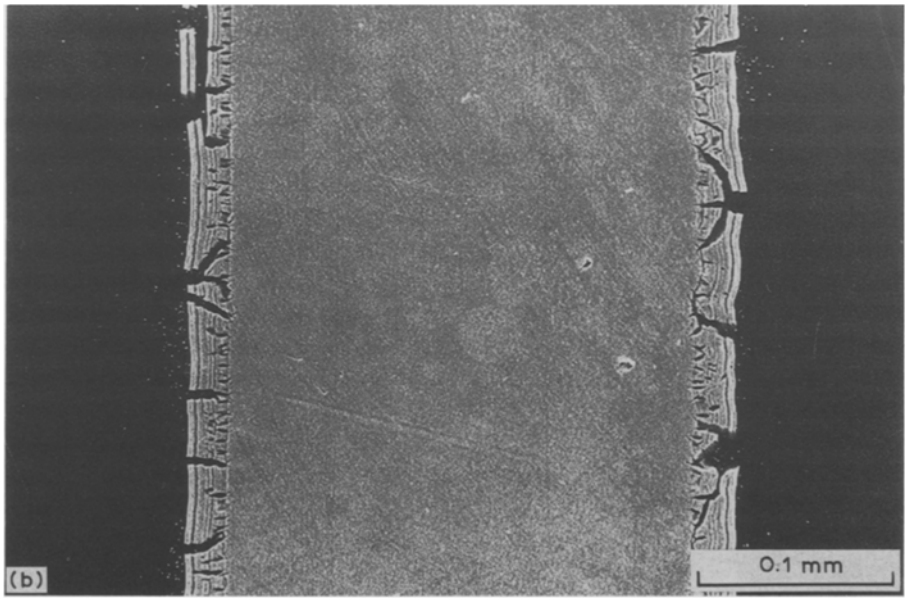

Fig. 7. (a) and (b) Correlation of potential–time profiles during Ni/Zn deposition and stratification of leached Raney-nickel coatings (electrodes 11 and 17). (——) $-E$/mV, (– – –) T/°C, (· · ·) pH and (–·–·–·–) $-i$/mA cm^{-2}.

Table 4. Overpotentials of the four selected electrodes

Electrode No.†	*250* /mA cm^{-2}	*500* /mA cm^{-2}	*1000* /mA cm^{-2}	*a**‡ /cm^2 cm^{-2}
11	−55	−82	−111	$4 \cdot 10^3$
17	−63	−90	−113	$7 \cdot 10^3$
9	−110	−180	−317	$4 \cdot 10^3$
7	−114	−186	−294	$9 \cdot 10^2$

† Electrodes operated initially over a period of 650 h at c.d. 250 mA cm^{-2} at 90 °C in 40 wt % KOH.
‡ Specific inner surface of electrodes (a^*): i.e. inner surface per 1 cm^2 of geometric electrode area.

the higher is the relative amount of non leachable zinc. Figure 6 depicts typical semilogarithmic current–voltage curves for cathodic hydrogen evolution measured at a non-activated nickel electrode and the current–voltage curves of four specimens of Raney-nickel activated cathodes obtained by codeposition of nickel zinc from acidic solutions. The activated specimens had been operated initially for 650 h at a cathodic current density of 250 mA cm^{-2}.

Table 4 shows the overpotentials measured at 100 °C in 40 wt % KOH at current densities of 250, 500 and 1000 mA cm^{-2} (*cf.* [18]). The electrodes are ordered in Table 4 according to decreasing catalytic activity; clearly electrode No. 11 is the electrode of highest activity. The last column of Table 4 contains the specific inner surface a^* of the electrodes (i.e. inner surface per 1 cm^2 of geometric electrode area). There is no evident correlation between the inner surface of the different catalyst coatings and the catalytic activity of the electrodes. The most active electrode (No. 11) has only half as much specific inner surface than the poorest one of the four selected electrodes. This lack of correlation may be attributed to morphological features of the coating.

5. Discussion

5.1. *Tertiary electrode structure and effective catalytic activity*

In Figs 7(a) and (b) and 8(a) and (b) microscopic cuts of the two best electrodes, No.'s 11 and 17, are correlated with the potential/current density–time profiles observed during electrolysis for their cathodic deposition.

Evidently the potential fluctuations, which occurred in the course of the deposition, reflect in a layered structure of the leached deposit. This layering is caused by significantly different porosities of the different strata, brought about by different zinc contents

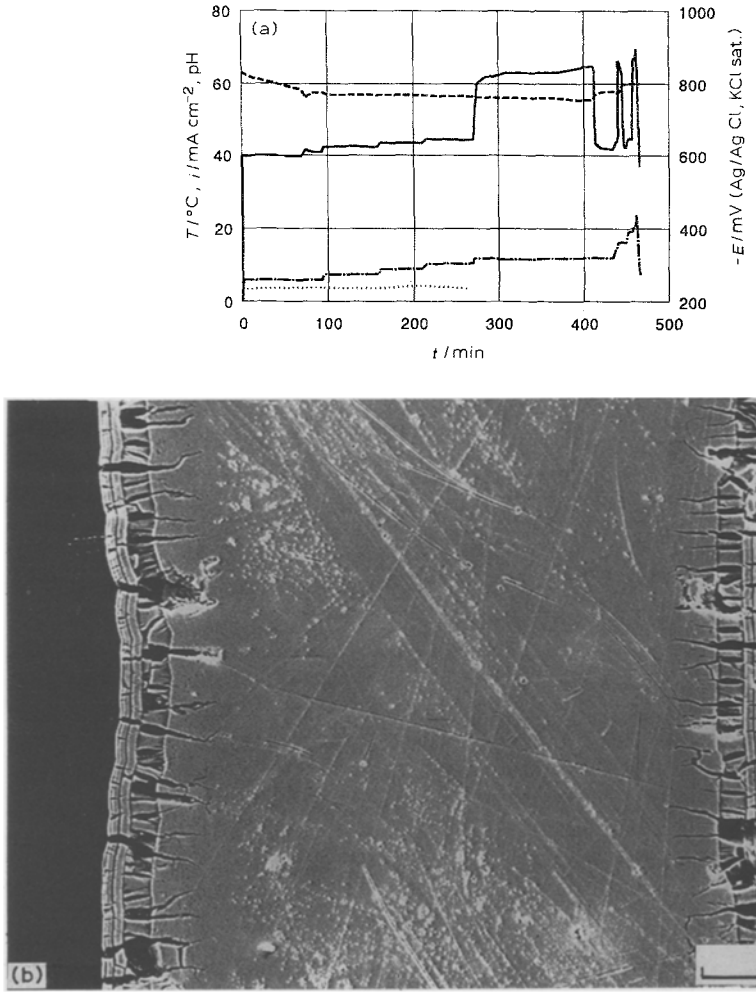

Fig. 8. As for Fig. 7.

of the precursor alloy layers obtained at higher cathodic potential (−900 mV, approx. 80% zinc, leachable alloy) and at lower potential (−600 mV, approx. 20% zinc, unleachable alloy), respectively.

Common to the specimens, No.'s 11 and 17, representing the most active coatings, is that at the end of the electrolysis there occurred repeatedly, a return to lower potentials resulting in a lower zinc content of the respective uppermost layer or layers. Below these low content zinc layers there exists in all cases a number of layers of a high zinc content which are converted to the most active form of catalyst by leaching. They shrink considerably, in all three dimensions, during caustic leaching, due to removal of the zinc from the lattice of the γ δ-phase. Shrinking can be clearly identified in the micrographs since it leads to formation of voids. The mechanical stability of the coatings, prepared from acidic solutions, is influenced by the thickness and the number of layers with low zinc content in the coatings. Although the uppermost layers, layers with a low zinc content in specimens 11 and 17, are not leachable they are divided by cracks.

These cracks even extend into the massive nickel support. They are due to shrinking of the coating which, during caustic leaching of zinc, looses approximately 40% of the initial volume of the nickel/zinc alloy [13]. The formation of these cracks is vital to higher utilization of the Raney-nickel because cracks, being filled with electrolyte, render a greater part of the internal surface of the Raney-nickel accessible to electrochemical gas evolution, than would be accessible in undivided, closed Raney-nickel layers. As shown in the first publication of this series by theoretical consideration [10], only a small fraction of the internal surface of Raney-nickel coatings is used if the coatings are not divided by cracks. Numerous cracks, as generated by leaching, lead to sufficiently short diffusion paths of homogeneously dissolved hydrogen for the fastest release of the gas and for avoiding excessive hydrogen accumulation and concentration polarization in the micropores. They further facilitate the release of gas bubbles.

It is the essential result of this investigation that coating stratification, together with cracks developed during caustic leaching of stratified precursor alloys, determine their morphology and effective catalytic activity to an unexpected extent which is not easy to control. The morphology determines the extent to which the internal surface of the Raney-nickel catalyst can contribute to cathodic H_2-deposition and the effective catalytic activity of the coating.

References

[1] J. Freel, W. J. M. Pieters and R. B. Andersen, *J. Catalysis* **14** (1968) 247–56.
[2] H. Wendt, 'Electrochemical Hydrogen Technologies', Elsevier, Amsterdam (1990), p. 39.
[3] K. Lohrberg and P. Kohl, *Electrochim. Acta* **29** (1984) 1557.
[4] T. A. Liederbach, A. M. Greenberg and V. H. Thomas, in 'Commercial applications in Chlorine cells', in 'Modern Chloralkali Technology' (edited by M. O. Coulter), Ellis Horwood, Chichester (1980), p. 145.
[5] J. Divisek and H. Schmitz, *Int. J. Hydrogen Energy* **15** (2), (1990) 105–14.
[6] J. Divisek, H. Schmitz and J. Mergel, *Chem.-Ing.-Technik* **32** (1980) 465.
[7] H. Wendt, *op. cit.* [2], p. 145.
[8] J. Divisek and H. Schmitz, *Int. J. Hydrogen Energy* **7** (9), (1982) 703–710.
[9] Lurgi, *Express Information D*, 1084/11.80.
[10] S. Rausch and H. Wendt, *J. Appl. Electrochem.*submitted for publication.
[11] J. Divisek, J. Mergel and H. Schmitz, *J. Appl. Electrochem.* **22** (1992) 705–10, 711–16.
[12] K. Alrust, Diplomarbeit, TH Darmstadt (1990).
[13] H. Wendt, H. Hofmann and V. Plzak, *Mater. Chem. Phys.* **22** (1989) 27–49.
[14] D. E. Hall, *Plat. Surf. Finish.* **70** (1983) 59.
[15] H. Fukushima, T. Akiyama and K. Higashi, *Metallwiss. u. Technik* **70** (1988) 242.
[16] M. Hansen, Constitution of binary alloys, 2nd ed., K. Anderko ed., McGraw-Hill, New York (1968) p. 1060.
[17] Th. Reeg, Diplomarbeit, TH Darmstadt (1990).
[18] H. Wendt and V. Plzak, *Electrochim. Acta* **28** (1), (1983) 27.